Soft Matter

PAPER

View Article Online
View Journal | View Issue

Cite this: *Soft Matter*, 2014, **10**, 911

Phenylboronate-diol crosslinked glycopolymeric nanocarriers for insulin delivery at physiological pH†

Qianqian Guo,[a] Zhongming Wu,[b] Xinge Zhang,*[a] Lei Sun[a] and Chaoxing Li[a]

Received 21st September 2013
Accepted 14th November 2013

DOI: 10.1039/c3sm52485j

www.rsc.org/softmatter

Research into polymers with glucose-sensitivity in physiological conditions has expanded recently due to their therapeutic potential in diabetes. Herein, to explore the glucose-responsive properties of a new polymer under physiological conditions, we synthesized an amphiphilic block glycopolymer based on phenylboronic acid and a carbohydrate, which was named poly(D-gluconamidoethyl methacrylate-*block*-3-acrylamidophenylboronic acid) (*p*(AAPBA-*b*-GAMA)). Based on the cross-linking between the diol groups of the carbohydrates and phenylboronic acid, the glycopolymers self-assembled to form nanoparticles (NPs). The glucose-sensitivity was revealed by the swelling behavior of the NPs at different glucose concentrations and was found to be dependent on the glucose level. The morphology of the NPs revealed by transmission electron microscopy showed that the NPs were spherical in shape with good dispersity. The cell viability of the NPs investigated by MTT assay was more than 90%, indicating that the glycopolymers had good cytocompatibility. Insulin could be loaded onto the glycopolymer NPs with high efficiency (up to 10%), and insulin release increased with enhancement of the glucose level in the medium. Such a glucose-responsive glycopolymer is an excellent candidate that holds great potential in the treatment of diabetes.

1. Introduction

Insulin-dependent diabetes is a serious disease affecting many people in the world. Currently, the treatment for diabetes requires persistent monitoring of blood glucose levels and multiple daily insulin injections.[1] This provides some control of the diabetic state, but this is far from the physiologic regulation achieved by a normally functioning pancreas and results in long-term complications, including cardiovascular disease, nephropathy, cataracts, retinopathy, and skin ulcers.[2,3] Great efforts have been devoted to investigating a system that is capable of consistently delivering accurate dose of insulin in response to glucose level changes.[4–6] For example, Gu *et al.* developed an artificial "closed-loop" system that could mimic pancreas activity and release insulin in response to glucose level changes. The self-regulating system could release insulin at basal release rates under normoglycemic conditions and at higher rates under hyperglycemic conditions.[5,6] Thus, one expedient strategy is to develop glucose-responsive materials to be utilized in a self-regulated insulin delivery system. Among three kinds of typical glucose-responsive materials,[7–9] phenylboronic acid and its derivatives are versatile enough to be used in different designs and are more stable than protein-based systems (glucose oxidase and concanavalin A),[10] have attracted great interest.

It is well known that phenylboronic acid and its derivatives have a specific covalent binding interactions with diol units, such as glucose,[11] and an important property of phenylboronic acid compounds in aqueous solution is that they are equilibrium between an uncharged and a charged form.[12,13] The charged phenylboronic acid is well known to form a stable complex with glucose, which lays the foundation for the glucose-responsiveness of phenylboronic acid-containing materials. However, phenylboronic acid and its derivatives are kinds of weak acids with a pK_a of 8.2 $\sim$ 8.6 (ref. 14 and 15) and most of the phenylboronic acid-based materials reported demonstrate maximum glucose-sensitivity at pH = 9 $\sim$ 10. Thus, significant efforts have been focused on decreasing the pK_a of phenylboronic acid-based glucose-responsive materials and enhancing their sensitivity to glucose at physiological pH.[16–28] Based on this object, Wang *et al.* described glucose-responsive micelles from the self-assembly of poly(ethylene glycol)-*b*-poly(acrylic acid-*co*-acrylamidophenylbornic acid) that could be applied to control insulin release at pH 7.4.[16] Matsumoto *et al.* introduced novel phenylborate derivatives,

[a]*Key Laboratory of Functional Polymer Materials of Ministry Education, Institute of Polymer Chemistry, Nankai University, Tianjin 300071, China. E-mail: zhangxinge@nankai.edu.cn; Fax: +86-22-23505598; Tel: +86-22-23501645*

[b]*2011 Collaborative Innovation Center of Tianjin for Medical Epigenetics, Key Laboratory of Hormones and Development (Ministry of Health), Metabolic Diseases Hospital, Tianjin Medical University, Tianjin 300070, China*

† Electronic supplementary information (ESI) available. See DOI: 10.1039/c3sm52485j

4-(1,6-dioxo-2,5-diaza-7-oxamyl)phenylboronic acid, with a pK_a of approximately 7.8 into a polymer as a glucose-sensing moiety, and the polymer displayed glucose-sensitivity at physiological pH.[23] Wu *et al.* also prepared a multifunctional hybrid nanogel with optical glucose sensing and controlled insulin release at physiological pH.[26] Recently, Kim *et al.* studied a monosaccharide-responsive system with the block copolymers self-assembling into a variety of nanostructures that exhibited monosaccharide-responsive disassembly in a neutral-pH medium and encapsulated insulin could be released from the polymersomes only in the presence of sugar under physiologically relevant pH conditions.[28]

However, a disadvantage of boronic acid-containing compounds is that they have some degree of cytotoxic activity.[29,30] To overcome the problem, it is necessary to introduce biocompatible compounds. Our previous work demonstrated that such a copolymer system composed of 3-acrylamidophenylboroniccid (AAPBA) and carbohydrate was devoted to decreasing the pK_a and improving the biocompatibility of phenylboronic acid.[31–37] The initial strategy involved the utilization of amino glucose to lower the pK_a of AAPBA *via* the free-radical polymerization, and the results showed that this copolymer, as glucose-sensitive matrix, had excellent potential for controlled insulin release.[31] Additionally, to enhance the loading capability of drug, we prepared a kind of core–shell hybrid nanoparticles with pH-gated and glucose-sensitivity that was utilized in controlling insulin release.[35] To further explore the *in vivo* application of the glucose-sensitive polymer, we designed and prepared injectable and glucose-sensitive nanogels based on poly(*N*-isopropylacrylamide), dextran and poly(3-acrylamidophenylboronic acid) and found that the nanogels decreased the blood glucose levels in diabetic rats and maintained 51% of the baseline level for almost 2 h.[36] Based on above-mentioned results, the introduction of the carbohydrate into polymers containing phenylboronic acid could not only improve the hydrophilicity and biocompatibility of the polymer but also decrease the pK_a of phenylboronic acid-containing materials.

To further investigate the structure–property relationship, herein, we synthesized new glucose-responsive diblock glycopolymers *p*(AAPBA-*b*-GAMA), comprised of AAPBA and D-gluconamidoethyl methacrylate (GAMA) by reversible addition-fragmentation chain transfer (RAFT) polymerization. The AAPBA endowed the glycopolymers with glucose-sensitivity, while GAMA, a kind of synthetic carbohydrate monomer, was a renewable source and introduced to reduce the toxicity and decrease the pK_a of AAPBA. Since the amphiphilic polymers can self-assemble into nanoparticles with a core–shell structure, the formation of the nanoparticles was investigated, and the *in vitro* release of insulin in response to glucose changes was further evaluated.

2. Materials and methods

2.1. Materials

3-Aminophenylboronic acid monohydrate was purchased from Nanjing Kangmanlin Chemical Industry Co. Ltd (Nanjing, China). Acryloyl chloride was prepared by refluxing acrylic acid and thionyl chloride at 75 °C for 8 h and freshly distilled before used, and methacryloyl chloride was obtained in a similar method at 90 °C. 2-Dodecylsulfanylthiocarbonylsulfanyl-2-methylpropionic acid (DMP) was synthesized according to the method as previously reported.[38,39] D-Gluconolactone and D-glucose were supplied by Tianjin no. 1 Chemical Reagent Factory (Tianjin, China). 2,2′-Azobisisobutyronitrile (AIBN) was recrystallized twice from ethanol and dried in vacuum. Pure crystalline porcine insulin was purchased from Xuzhou Wanbang Biochemical Co. Ltd. (Xuzhou, China). 3-[4,5-Dimethylthiazol-2-yl]-2,5-diphenyltetrazolium bromide (MTT) was obtained from Beyotime Institute of Biotechnology (Nantong, China). Other reagents were of analytical grade and used as received.

2.2. Synthesis of glycopolymer based phenylboronic acid

2.2.1. Synthesis of AAPBA. AAPBA was prepared using the modified method described by Lee *et al.*[40] Briefly, 3-aminophenylboronic acid monohydrate (5.0 g, 32.2 mmol) and sodium bicarbonate (5.0 g, 59.5 mmol) were dissolved in 45 mL of a water and tetrahydrofuran (THF) mixed solution (v/v, 2 : 1), and cooled in an ice bath. Acryloyl chloride (5 mL, 62.5 mmol) was added drop-wise into the mixture solution with stirring over a period of 1 h. Then the reaction mixture was preformed for another 2 h at room temperature. The obtained solution was extracted with acetic ether and the organic phase was concentrated to obtain a dry crude product. Subsequently, the crude product was recrystallized in 80 mL of hot water (90 °C). The resulting crystals were filtered, washed with water, dried under vacuum, and isolated in 52% yield.

2.2.2. Synthesis of poly(3-acrylamidophenylboronic acid) (pAAPBA). pAAPBA was synthesized by RAFT polymerization using a previously method reported.[41] The polymerization was carried out by using AAPBA as the monomer, DMP as the RAFT agent, AIBN as the initiator, and *N*,*N*-dimethylformamide (DMF)–water (v/v, 19 : 1) as the solvent. The mixture solution was sealed in a 50 mL reaction tube and purged with nitrogen for 30 min. Then the tube was transferred to a preheated oil bath at 70 °C. The reaction was quenched after 10 h by cooling in ice water for 5 min. The resultant polymer was isolated by removing the solvent, precipitating into diethyl ether, washing with acetone and drying under vacuum. By changing the feed molar ratio of AAPBA to DMP (100 : 1, 150 : 1 and 200 : 1), three different homopolymers were obtained, marked as pAAPBA100, pAAPBA150 and pAAPBA200, respectively.

2.2.3. Synthesis of GAMA

2.2.3.1. Synthesis of ethanolamine hydrochloride. The ethanolamine hydrochloride was synthesized according to a previous report.[42] A 37% (w/w) hydrochloric acid solution (71 mL, 0.875 mol) was added during 2 h to a mixture of ethanolamine (53 mL, 0.875 mol) and water (100 mL) under stirring at 90 °C. After being incubated for 1 h at 105 °C, the mixture was concentrated, precipitated in anhydrous ether and dried under vacuum at 40 °C with a yield of 95%.

2.2.3.2. Synthesis of 2-aminoethyl methacrylate (AMA). AMA was synthesized using a previously reported protocol.[43]

Ethanolamine hydrochloride (65.0 g, 0.67 mol), methacryloyl chloride (100 mL, 0.96 mol), and hydroquinone (0.5 g) were added to a three-necked round-bottomed flask fitted with a condenser. The mixture was heated in an oil bath to 93 °C under a nitrogen atmosphere for 1 h with vigorously stirring, and then further maintained at 70 °C for 2 h. The mixture was cooled to 40 °C and 150 mL of THF was added. The solution was then dropped slowly to cold 600 mL of *n*-pentane and the formed creamy white precipitate was isolated by filtration, washed well with *n*-pentane, and dried under vacuum. The crude product was recrystallized using an ethyl acetate and 2-propanol mixture (v/v, 7 : 3) and isolated in its hydrochloride salt form. The yield was 60%.

2.2.3.3. Synthesis of GAMA. GAMA was prepared according to the previous report.[43] Briefly, D-gluconolactone (10 g, 56.2 mmol) was dissolved in 100 mL of methanol. AMA (16.0 g, 96.6 mmol), hydroquinone (0.1 g) and triethylamine were added, and the reaction solution was stirred at 20 °C for 5 h. The obtained mixture was then concentrated and precipitated into either excess dichloromethane or 2-propanol. After filtered off, washed, and dried under vacuum, the pure product was obtained with the yield of 45%.

2.2.4. Synthesis of *p*(AAPBA-*b*-GAMA). RAFT copolymerization was performed at [GAMA] : [pAAPBA macroRAFT] : [AIBN] = 50 : 1 : 1. By using GAMA as a monomer, the homopolymer pAAPBA as a macroRAFT agent, AIBN as the initiator, and DMF–water (v/v, 19 : 1) as the solvent, the reaction system was placed in a preheated oil bath at 70 °C for 12 h following nitrogen purging for 30 min. The polymerization was quenched by cooling in ice water for 5 min. The resulting polymer was isolated by washing with water and acetone three times, respectively, and drying under vacuum. By changing the ratio of pAAPBA to GAMA, three distinct glycopolymers were prepared and named as *p*(AAPBA2-*b*-GAMA1), *p*(AAPBA3-*b*-GAMA1) and *p*(AAPBA4-*b*-GAMA1).

2.3. Characterization of the glycopolymers

^{1}H NMR spectra were recorded at room temperature using a Varian Unity-plus 400 NMR spectrometer. FT-IR spectra were recorded on a Fourier Transform Infrared Spectrometer (FTS-6000, Bio-Rad Co.) using a KBr tablet containing the sample powder at a resolution of 8 cm^{-1}.

2.4. Preparation of *p*(AAPBA-*b*-GAMA) NPs

p(AAPBA-*b*-GAMA) NPs were prepared according to a previously reported method.[31] 10 mg of *p*(AAPBA-*b*-GAMA) was dissolved in 2 mL of a mixed solvent containing dimethyl sulfoxide (DMSO) and water (v/v, 1 : 1) and 20 mL of water was then added dropwise to the solution under stirring. The resulting opalescent solution was transferred to a dialysis tube (MWCO 3500) and dialyzed against water for 24 h. The organic solvent was removed by replacing water every 3 h during the dialyzing process. After freeze-drying the suspension, blank NPs were obtained.

The insulin-loaded NPs were prepared with a similar method by using 500 μg mL^{-1} of insulin solution. After dialysis for 24 h, the insulin-loaded NPs suspension was centrifuged at 12 000 rpm for 20 min. The amount of free insulin in the supernatant was monitored by the Bradford method using a UV spectrometer (Shimadzu UV-2550) at 595 nm.[44] Insulin encapsulation efficiency (EE) and loading capacity (LC) were calculated using the following equations:

$$\mathrm{EE}\% = \frac{\text{total insulin} - \text{free insulin}}{\text{total insulin}} \times 100 \quad (1)$$

$$\mathrm{LC}\% = \frac{\text{total insulin} - \text{free insulin}}{\text{NPs weight}} \times 100 \quad (2)$$

2.5. Characterization of NPs

The hydrodynamic diameter (D_H) and size distribution of the NPs were characterized by dynamic light scattering (DLS) using a Malvern Zetasizer Nano S apparatus equipped with a 4.0 mV laser operating at λ = 636 nm. All measurements were performed at a scattering angle of 90°. The morphological characteristics of the NPs were determined by transmission electron microscopy (TEM, Philips EM400ST). Samples were placed on copper grids coated with Formvar films for observing under TEM.

2.6. Reversible glucose sensitivity of the NPs

p(AAPBA4-*b*-GAMA1) NPs were chosen to be the representative nanoparticles to evaluate the reversible glucose sensitivity. The blank NPs were treated with 3 mg mL^{-1} glucose in PBS followed with dialysis against water for 24 h. Subsequently, the NPs after dialysis were further exposed to 3 mg mL^{-1} glucose. The size of the NPs was measured by DLS.

2.7. Cell viability

Cell viability of *p*(AAPBA-*b*-GAMA) was evaluated by using NIH 3T3 cells. The cell line grew at 5% CO_2, 95% O_2 in Dulbecco's modified Eagle's medium (DMEM, Gibco). The cells were seeded into 96-well plates at 10 000 cells per well and were incubated for 24 h. 100 μL of glycopolymer NPs suspension with a range of concentrations from 25 to 500 μg mL^{-1} was added into the plates for further incubation after removal of the cell culture medium. After 24 h, the culture medium and 20 μL of MTT were added to replace the mixture in each well and the cells were incubated for a further 4 h. After removal of the culture medium and MTT, 100 μL of DMSO was added to each well to dissolve the formazan crystals under low-speed shaking for 10 min, the absorbance was measured on a microplate reader at 495 nm. The cell viability was determined as a percentage of the negative control; untreated cells were used as the negative control and their proliferation rate was set as 100%.

2.8. *In vitro* release study

In vitro release of different NPs was investigated by incubating 6 mg of insulin-loaded NPs at 37 ± 0.5 °C with 2 mL of pH 7.4 phosphate buffer solution (PBS, 0.1 M) containing different

glucose concentrations (0, 1 and 3 mg mL^{-1}) under shaking (100 rev per min). Insulin release from *p*(AAPBA4-*b*-GAMA1) NPs was also achieved by altering the glucose concentration from 0 to 3 mg mL^{-1} in the same medium. The NPs were incubated in free glucose for the first 9 h and then glucose was added to obtain a final concentration of 3 mg mL^{-1}. At a predetermined time, samples were centrifuged at 12 000 rpm for 5 min and 100 μL of supernatant was withdrawn and fresh buffer solution was added. The amount of free insulin was monitored using the Bradford method. Each sample was analyzed in triplicate and the results were reported as mean ± standard deviation ($n = 3$).

2.9. Circular dichroism spectroscopy

The stability of the released insulin was determined by analysis of the conformation of released insulin using circular dichroism (CD) and the resulting spectrum was compared to that of standard insulin. The standard insulin solution was prepared in pH 7.4 PBS to a final concentration of 0.1 mg mL^{-1}. CD measurements were performed on a Jasco J-715 CD spectropolarimeter at 25 °C with a cell length of 0.1 cm. For the far-UV CD spectra, samples were scanned from 190 to 260 nm and accumulated 10 times, at a resolution of 1.0 nm and scanning speed of 100 nm min^{-1}. All CD data are expressed as mean residue ellipticity.[45]

3. Results and discussion

3.1. Synthesis and characterization of *p*(AAPBA-*b*-GAMA) glycopolymers

p(AAPBA-*b*-GAMA) glycopolymers were synthesized *via* a sequential RAFT polymerization method (Scheme 1). First, pAAPBA homopolymers were prepared by RAFT of AAPBA using DMP as initiator. Then, *p*(AAPBA-*b*-GAMA) diblock glycopolymers were prepared by subsequent RAFT using pAAPBA as macroRAFT. By changing the ratio of pAAPBA to GAMA, three distinct glycopolymers were obtained. During the synthetic process, we found that the glycopolymer was difficult to dissolve as the ratio of GAMA to AAPBA increased. Importantly, GAMA was introduced to decrease the pK_a of AAPBA (8.2) to 7.5. The pK_a of the glycopolymer was determined using a pH meter and the results are shown in the Supporting Information.† Fig. 1 showed the FT-IR spectra of pAAPBA and *p*(AAPBA-*b*-GAMA). In comparison with pAAPBA, *p*(AAPBA-*b*-GAMA) maintained the typical absorption of pAAPBA described as follows. There was a broad absorption band in the range of 3200 to 3600 cm^{-1}, which was due to the hydrogen bonds formed between hydroxyls of the carbohydrate moieties and N–H stretching of amide groups. The peak band at 1666 cm^{-1} was assigned to C=O stretching (amide I band) while the amide II band attributed to N–H bending vibration of a secondary amide resulting in an absorption band of 1539 cm^{-1}. The band in the range of 1200 to 1000 cm^{-1} corresponded to C–O stretching of the alkoxy bond in the carbohydrate moieties. Besides, a

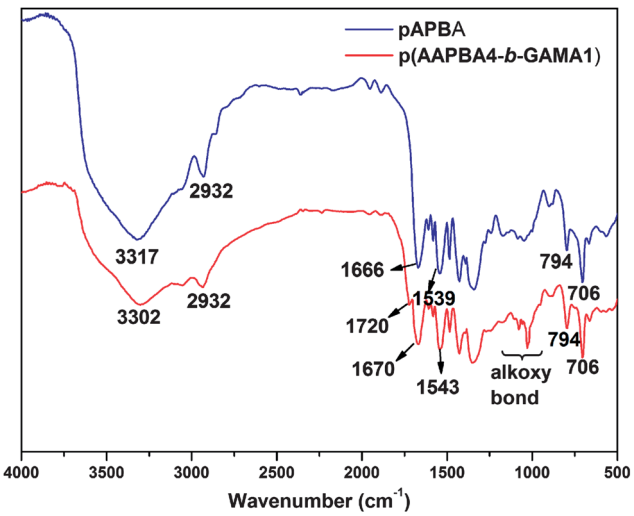

Fig. 1 FT-IR spectra of *p* AAPBA and p(AAPBA-*b*-GAMA).

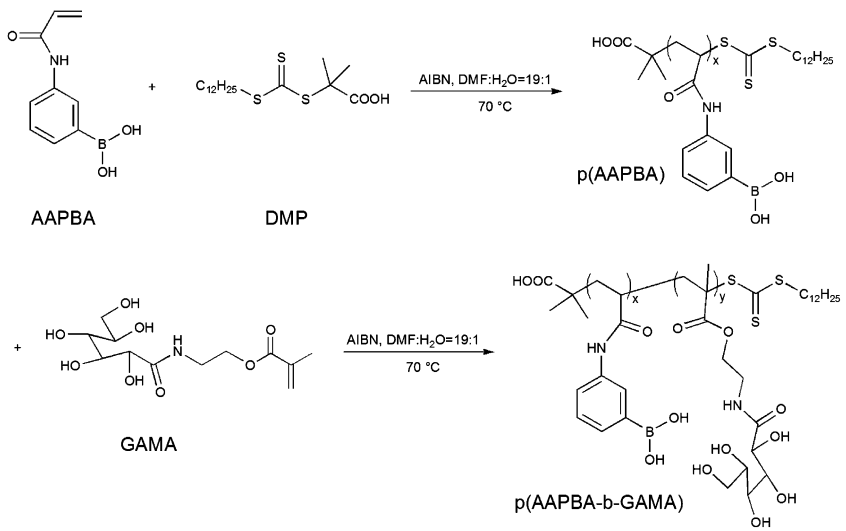

Scheme 1 Synthesis of the block amphiphilic glycopolymer *p*(AAPBA-*b*-GAMA).

new typical absorption appeared at 1720 cm^{-1} attributing to the ester groups stretching vibration in GAMA units. Except for the broad absorption band and C–O stretching band that reflected the presence of carbohydrate moieties, typical peaks of the phenyl ring in AAPBA in the 1500 to 1300 cm^{-1} region and absorption peaks at 794 and 706 cm^{-1} were observed. ^{1}H NMR spectra of AAPBA, pAAPBA, and *p*(AAPBA-*b*-GAMA) are shown in Fig. 2. Compared with the spectrum of AAPBA, it was observed in the spectrum of *p*(AAPBA-*b*-GAMA) that the resonance signals of phenyl-ring protons at 7.0 ~ 8.0 ppm were retained, but the resonance signals assigned to protons on the double bond completely disappeared. And new resonance signals also appeared in the range of 0.5 ~ 1.7 and 3.2 ~ 3.6 ppm, which were assigned to the protons from the sugar units, indicating that *p*(AAPBA-*b*-GAMA) copolymer was synthesized successfully.

3.2. Characterization of *p*(AAPBA-*b*-GAMA) NPs

The *p*(AAPBA-*b*-GAMA) NPs were prepared by nanoprecipitation method coupled with dialysis. *p*(AAPBA-*b*-GAMA) self-assembled to form NPs with a hydrophilic pGAMA corona and a hydrophobic pAAPBA core (Scheme 2). TEM photographs of *p*(AAPBA4-*b*-GAMA1) NPs in Fig. 3A clearly illuminate that the NPs were spherical shape with good dispersion. The results determined by DLS are shown in Fig. 4 and 5 and Table 1. Generally, the size of blank *p*(AAPBA-*b*-GAMA) NPs was in the range of 125 to 190 nm and exhibited a narrow size distribution, with a polydispersity index (PDI) between 0.090 and 0.186. The average D_H for the NPs *p*(AAPBA2-*b*-GAMA1), *p*(AAPBA3-*b*-GAMA1) and *p*(AAPBA4-*b*-GAMA1) were 129.2, 156.9 and 188.6 nm, respectively. It is shown in Fig. 5 that the size of the blank NPs had little change over 6 weeks, indicating that *p*(AAPBA-*b*-GAMA) NPs were stable in aqueous solution.

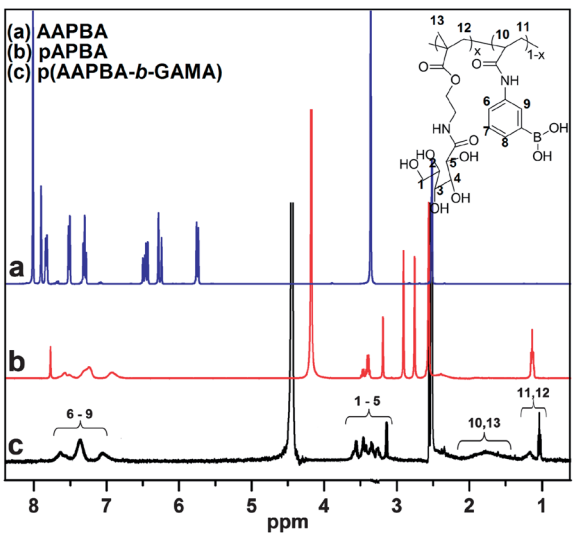

Fig. 2 ^{1}H NMR spectra of (a) AAPBA (DMSO-d_6); (b) pAAPBA (Methanol-d_4); and (c) *p*(AAPBA4-*b*-GAMA1) (the mixed solvent of DMSO-d_6 and D_2O).

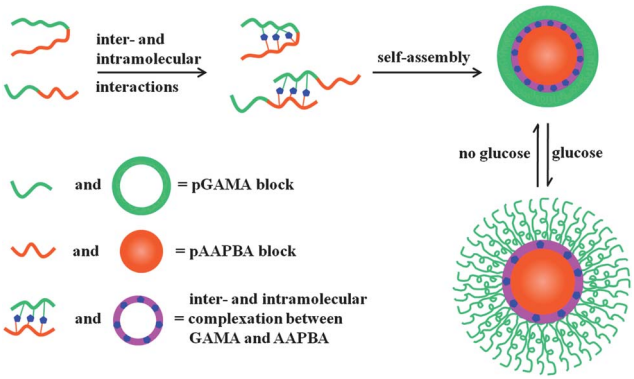

Scheme 2 Schematic representation of the *p*(AAPBA-*b*-GAMA) NPs formation.

3.3. The glucose sensitivity

The introduction of AAPBA groups endowed the resultant NPs with glucose sensitivity. It can be seen in Table 1 that all of the NPs appeared larger in size after treatment with 1 or 3 mg mL^{-1} glucose. The results in Fig. 3B show that *p*(AAPBA4-*b*-GAMA1) NPs increased to approximately 120 nm in size after treatment with 3 mg mL^{-1} glucose. Obviously, after glucose treatment, the size of the NPs became larger than that without glucose

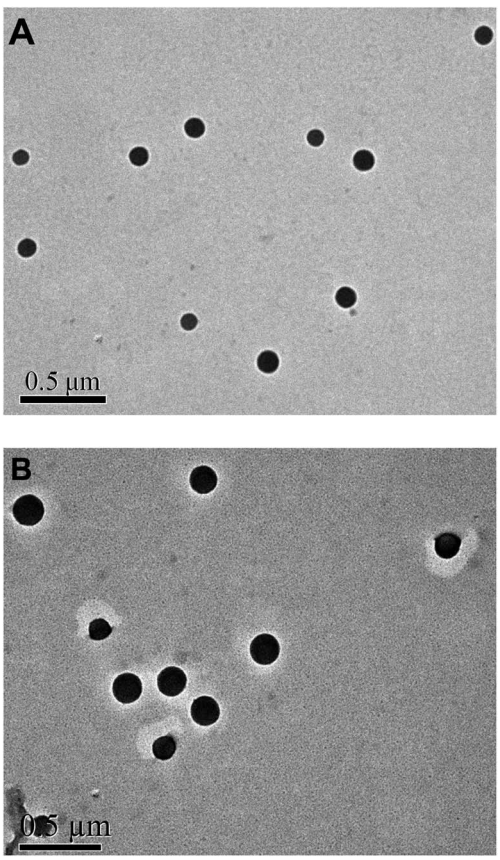

Fig. 3 TEM of *p*(AAPBA4-*b*-GAMA1) NPs before (A) and after (B) treatment with 3 mg mL^{-1} glucose.

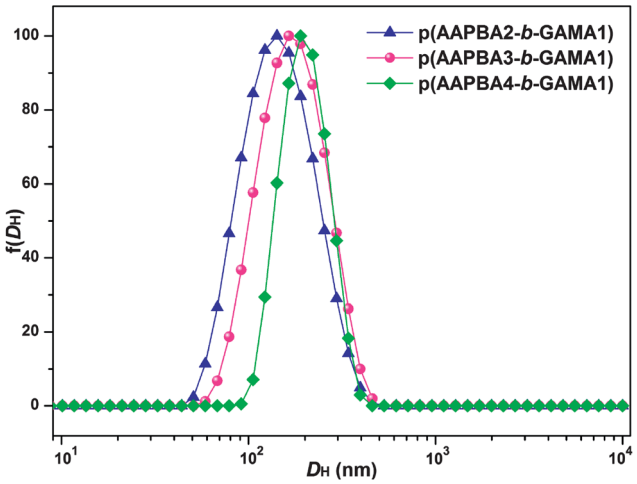

Fig. 4 Size distribution of blank *p*(AAPBA-*b*-GAMA)NPs in pH 7.4 PBS.

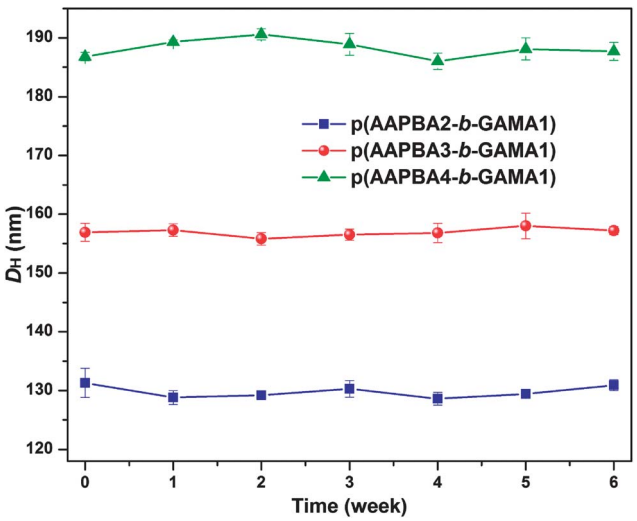

Fig. 5 The stability of blank *p*(AAPBA-*b*-GAMA) NPs in pH 7.4 PBS.

treatment. The swelling phenomenon indicates that the glucose exposure influenced the morphology of the NPs and *p*(AAPBA-*b*-GAMA) was responsive to glucose. Fig. 6 shows the values of I/I_0 *versus* time, and the inset showed the values of D_H *versus* glucose concentrations in pH 7.4 PBS. It is clearly shown that the values of I/I_0 decreased gradually as glucose concentration increased from 0 to 3 mg mL^{-1}, which was in accordance with an increase in the D_H for the three NPs. Noted that the decrement of the I/I_0 value was more in 3 mg mL^{-1} glucose than that in 1 mg mL^{-1}, which was attributed to more dissociation of NPs in higher glucose concentration. That the D_H increased with an increase of the glucose concentration significantly affected the swelling of NPs. This is due to the boronic ester linkages between the boronic acid-containing block copolymers with diols being dynamic-covalent, and the dynamic-covalent nature of the boronic ester allowed the linkage to reconfigure their structure in the presence of other diols that competed for bonding with the boronic acid competent. These results were agreement with those reported by the Sumerlin group.[46,47] Thus, the linkages could be induced to dissociate *via* competitive exchange reactions.

Fig. 7 showed the stimulation-responsiveness of *p*(AAPBA4-*b*-GAMA1) NPs in the presence of glucose. The NPs in the glucose free medium remained relatively stable during the determined time span. The results in Fig. 7A show that the light scattering intensity gradually reduced and subsequently levelled off with increasing glucose concentration over 24 h, that is, aggregate dissociation was highly dependent on the concentration of glucose, with higher concentrations leading to faster and more efficient dissociation. The glucose-responsiveness of the NPs with a lower concentration is shown in Fig. 7B. Compared to Fig. 7A with a higher NP concentration, aggregate dissociation was rapid and efficient for all concentrations of glucose. After the addition of glucose, I/I_0 reduced with the increment of glucose concentration due to the swelling and dissociation of NPs influenced by glucose concentration. After 16 h, the I/I_0 curves reached a plateau over zero which was ascribed to the cross-linking[48,49] and the homeostasis of the dissociation and association[16,50] between boronic acid derivatives and glucose in the solution.

The result of DLS monitoring in Fig. 8 showed the glycopolymers with reversible glucose sensitivity. The *p*(AAPBA4-*b*-GAMA1) swelled from 191.7 to 217.7 nm after the first treatment with 3 mg mL^{-1} glucose for 4 h, and then contracted to 193.0 nm, which was near to its original size after dialysis against water for 24 h. When treated with 3 mg mL^{-1} glucose for the second time, the NPs swelled to 220.1 nm, which was close to the first swelling size.

3.4. Insulin encapsulation and *in vitro* release

Insulin-loaded *p*(AAPBA-*b*-GAMA) NPs were prepared by adding insulin solution into *p*(AAPBA-*b*-GAMA) solution. The self-

Table 1 D_H and PDI of the NPs at various glucose concentrations measured by DLS

	Glucose concentration (mg mL^{-1})					
	0		1		3	
Samples	D_H (nm)	PDI	D_H (nm)	PDI	D_H (nm)	PDI
p(AAPBA2-*b*-GAMA1)	129.2 ± 1.243	0.186 ± 0.015	148.3 ± 1.942	0.167 ± 0.009	160.9 ± 1.212	0.124 ± 0.052
p(AAPBA3-*b*-GAMA1)	156.9 ± 1.546	0.162 ± 0.017	168.7 ± 1.408	0.154 ± 0.024	181.6 ± 2.076	0.111 ± 0.024
p(AAPBA4-*b*-GAMA1)	188.6 ± 2.041	0.090 ± 0.024	201.7 ± 1.967	0.095 ± 0.027	220.8 ± 2.328	0.097 ± 0.041

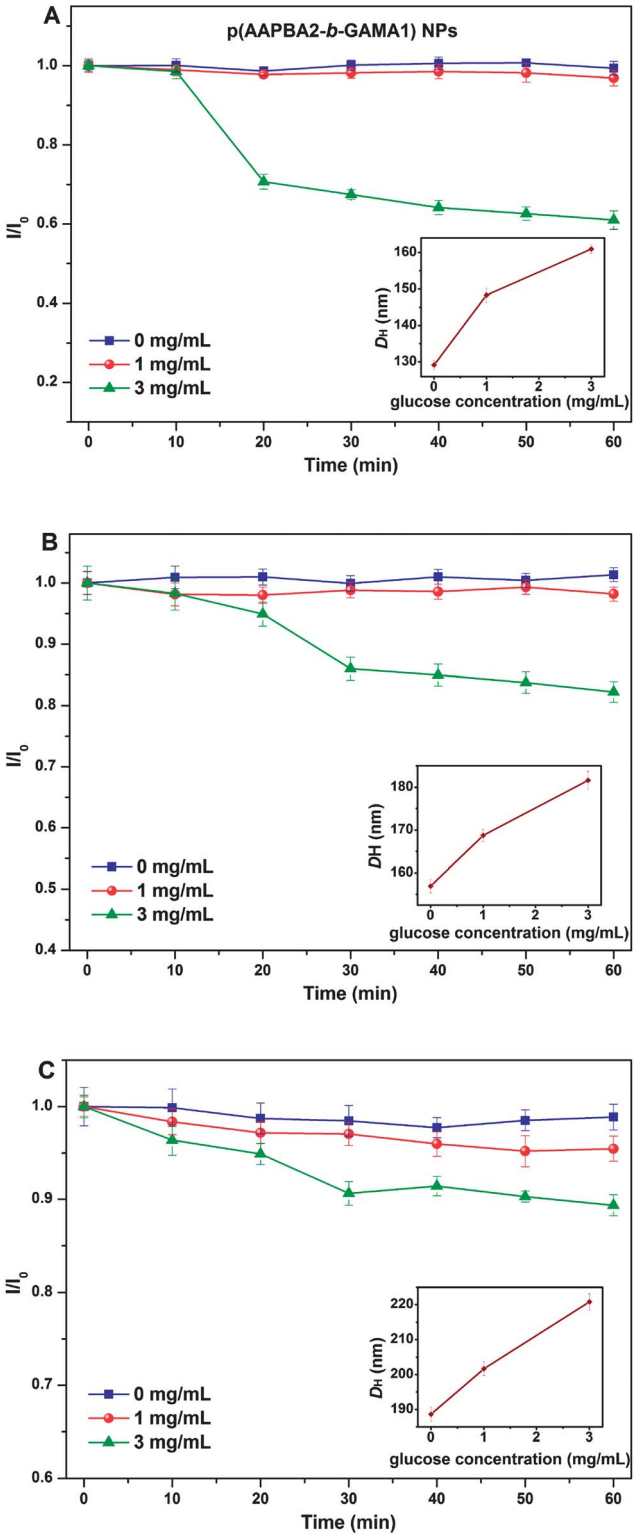

Fig. 6 Light scattering intensity of the glucose-response of 1 mg mL^{-1} of *p*(AAPBA-*b*-GAMA) NPs: (A) *p*(AAPBA2-*b*-GAMA1); (B) *p*(AAPBA3-*b*-GAMA1); (C) *p*(AAPBA4-*b*-GAMA1) and their light scattering intensity as a function of time in pH 7.4 PBS.

assembly process was affected by some kinds of interactions such as hydrophobic–hydrophilic interaction, electrostatic interaction, hydrogen bonding and other intermolecular

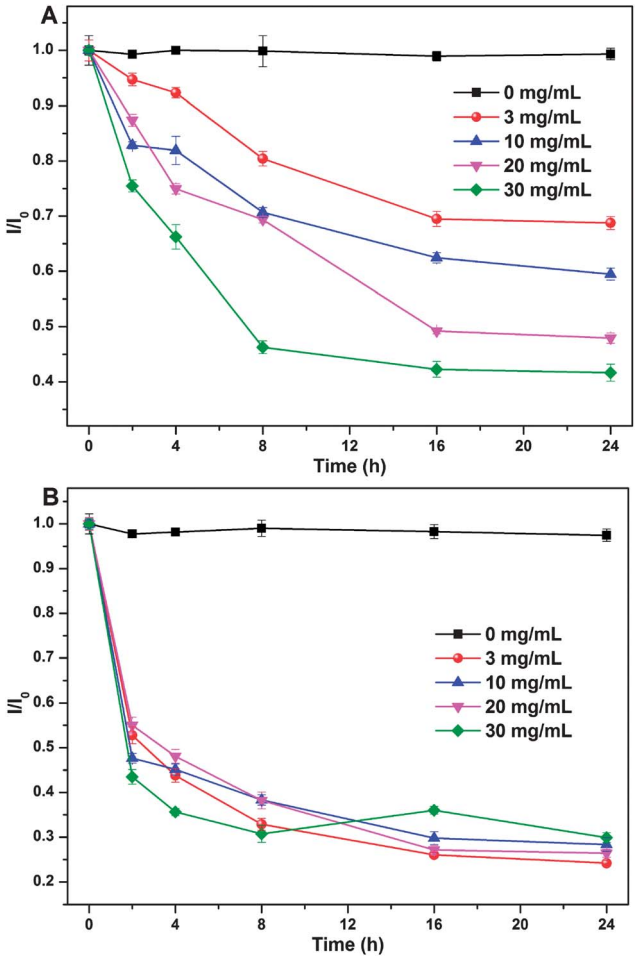

Fig. 7 Light scattering intensity of the glucose-responsiveness of two concentrations of *p*(AAPAB4-*b*-GAMA1) NPs in pH 7.4 PBS with different glucose concentrations in terms of light scattering intensity as a function of time: (A) 1 mg mL^{-1} and (B) 0.1 mg mL^{-1}.

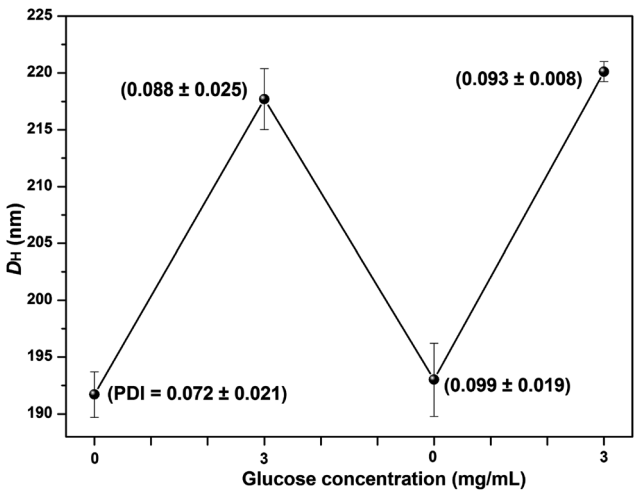

Fig. 8 Reversible glucose sensitivity of *p*(AAPBA4-*b*-GAMA1) NPs.

interactions. Insulin, a protein containing kinds of amino acids, has hydrophilic and hydrophobic residues and can form stable complexes due to these interactions.[51–53] Thus, when insulin was added into *p*(AAPBA-*b*-GAMA) solution and coupled with the amphiphilic glycopolymer, insulin can be loaded to the glycopolymer NPs with interactions of hydrogen bonding, van der Waals force and the hydrophilic–hydrophobic interaction. The results in Table 2 show that insulin was easily encapsulated into *p*(AAPBA-*b*-GAMA) NPs, and the LC of insulin was about 10% for all NPs. What's more, the EE of insulin increased from 53.2% to 63.8% with an increase of pAAPBA moieties. The possible reason for the high efficiency was the hydrophobic interaction between pAAPBA and insulin.

Fig. 9A exhibited the release profiles of insulin from drug-loaded *p*(AAPBA-*b*-GAMA) NPs upon exposure to 3 mg mL^{-1} glucose. The release displayed a burst release phase, indicating that some insulin was adsorbed onto the particle surface during the preparation of the NPs, and then rapidly diffused when the NPs came into contact with the release medium. Moreover, the burst insulin was higher, which was 20%, 16% and 12% for *p*(AAPBA2-*b*-GAMA1), *p*(AAPBA3-*b*-GAMA1) and *p*(AAPBA4-*b*-GAMA1), respectively. The release rate of insulin gradually decreased and the amount of insulin released after 48 h was 68%, 57% and 47% for *p*(AAPBA2-*b*-GAMA1), *p*(AAPBA3-*b*-GAMA1) and *p*(AAPBA4-*b*-GAMA1), respectively. As AAPBA content in *p*(AAPBA-*b*-GAMA) increased, more glucose-mediated association and relatively less dissociation occurred leading to a release rate of insulin from the NPs in the following order: *p*(AAPBA2-*b*-GAMA1) > *p*(AAPBA3-*b*-GAMA1) > *p*(AAPBA4-*b*-GAMA1), which was in accordance with the reported result.[16,50]

Fig. 9B showed the release profile of insulin in response to different glucose concentrations from drug-loaded *p*(AAPBA4-*b*-GAMA1) NPs. There was approximately 18.7% of insulin released in the glucose-free medium within 48 h, resulting from the insulin adsorbed onto the particle surface. As the glucose concentration increased from 0 to 3 mg mL^{-1}, the amount of insulin release enhanced significantly from 26% to 47%, which was ascribed to a greater association for 3 mg mL^{-1} glucose to the AAPBA moiety which is consistent with the results displayed in Fig. 6C. Further investigation on the release profile of *p*(AAPBA4-*b*-GAMA1) NPs was carried out by altering the glucose concentration from 0 to 3 mg mL^{-1}. After insulin release reached a plateau within the first 9 h in the glucose-free medium, glucose was added to obtain a final concentration of 3 mg mL^{-1}. The result in Fig. 9B shows that there was a significant increase in the amount of insulin release, which was dependent on the glucose concentration, suggesting the responsivity of the glycopolymers to glucose and the rapid insulin release upon exposure to glucose. Generally, insulin is injected into the patients before dinner so that the insulin can decrease the glucose level and avoid the occurrence of high blood sugar after dinner. In the present work, the time scales for insulin delivery are compatible with the patient's needs. Since the glycopolymer NPs deliver insulin in less than 30 min, they facilitate a decrease in the postprandial blood sugar of the patients.[54] Importantly, the glucose-sensitive carrier could control insulin release responding to the glucose levels in the blood, which avoids glucose fluctuations, and subsequently decreases the occurrence and development of complications. These self-regulated insulin delivery *in vitro* studies may have potential application for the treatment of diabetes.

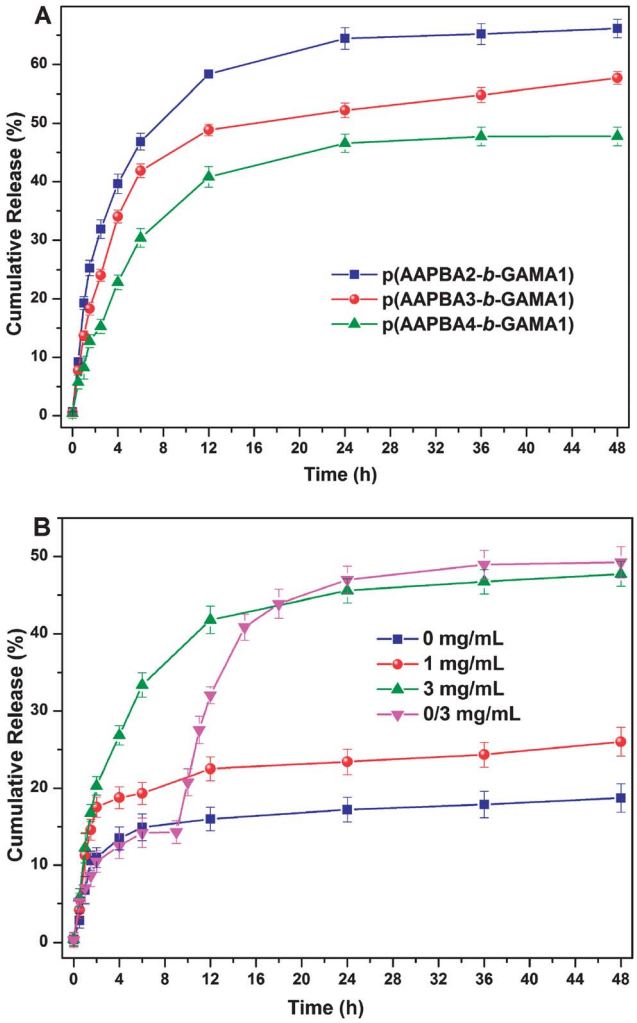

Fig. 9 *In vitro* cumulative release of insulin in pH 7.4 PBS from (A) *p*(AAPBA-*b*-GAMA) NPs at the glucose concentration of 3 mg mL^{-1}; (B) *p*(AAPBA4-*b*-GAMA1) NPs at various glucose concentrations (0, 1 and 3 mg mL^{-1}) and medium only for the first 12 h and then 3 mg mL^{-1}.

Table 2 EE and LC of the *p*(AAPBA-*b*-GAMA) NPs

Samples	EE (%)	LC (%)
p(AAPBA2-*b*-GAMA1)	54.20 ± 0.68	9.90 ± 3.94
p(AAPBA3-*b*-GAMA1)	57.19 ± 1.17	13.38 ± 1.88
p(AAPBA4-*b*-GAMA1)	63.76 ± 1.53	11.65 ± 4.47

3.5. Stability of the released insulin

CD spectroscopy was used to evaluate the conformational changes of insulin.[55,56] The far-UV-CD band at 208 nm primarily arises from an α-helix structure, while the band at 223 nm is for the β-structure. The ratio between both bands ($[\Phi]_{208}/[\Phi]_{223}$) can

be used to generate a qualitative measure of the overall conformational structure of insulin. In our study, the $[\Phi]_{208}/[\Phi]_{223}$ ratio for standard insulin and released insulin was 1.29 and 1.14, respectively. As indicated by the CD spectra (Fig. 10), no significant conformational change was observed for the insulin released from the NPs at pH 7.4 in comparison with standard insulin. Furthermore, the spectral characteristics indicate that the tertiary structure of released insulin has not been distorted.

3.6. Cell viability

It is important to verify the cytotoxicity of synthetic glycopolymers as phenylboronic acid and its derivatives have had cytotoxic activity in multiple cell lines. Fig. 11 shows the cytotoxicity of *p*(AAPBA-*b*-GAMA) NPs on NIH3T3 cells determined by the MTT method. The cells were exposed to the NPs suspensions from 25 to 500 μg mL^{-1} and the cells without pretreatment were used as a negative control group. After incubating for 24 h, the relative cell viability was higher than 90% for all of the glycopolymers, indicating that the presence of the glycopolymer did not negatively impact cell viability. The cell viability almost increased with decreasing AAPBA content in the glycopolymer. Overall, these results suggest that the carbohydrate moieties in the glycopolymers reduced the cytotoxicity and enhanced the glucose-sensitivity of the glycopolymers bearing phenylboronic acid, and that these NPs have a potential application for *in vivo* insulin delivery.

4. Conclusions

In this study, a new amphiphilic block glycopolymer based on phenylboronic acid and carbohydrate was synthesized. The glycopolymers could self-assemble to form stable spherical NPs with phenylboronate-diol crosslinked bond and exhibited glucose-sensitive behavior at physiological pH. The particle size increased in correlation with the glucose concentration, and the glucose sensitivity of the glycopolymer NPs was reversible. Insulin was encapsulated into the NPs with high loading capacity of approximately 10%. The release of insulin in response to glucose levels was revealed by the insulin release profiles. The biocompatibility of the glycopolymers bearing phenylboronic acid was improved by introduction of carbohydrate moieties, which gives the glycopolymers potential to be used in biomedical fields. In conclusion, the data indicate that the glycopolymers have the potential for use in a self-regulated insulin delivery system in the future.

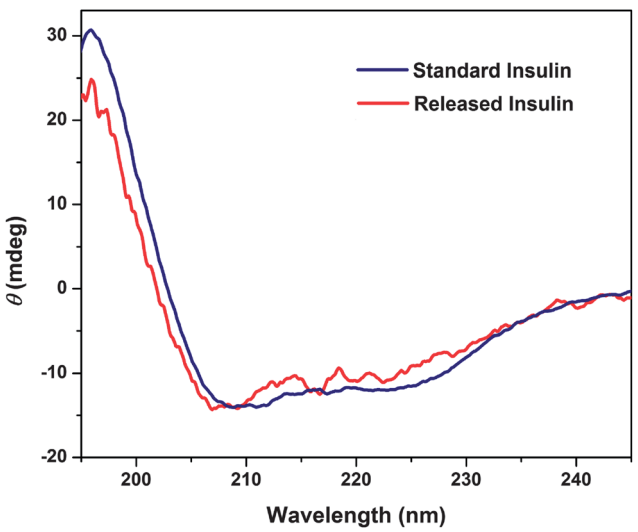

Fig. 10 UV-CD spectra of standard insulin and released insulin.

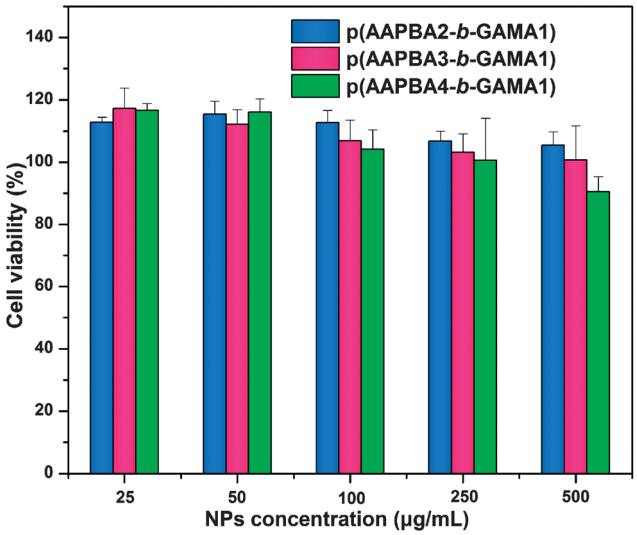

Fig. 11 Cell viability as a function of *p*(AAPBA-*b*-GAMA) NPs concentration by the MTT assay at 37 °C after the incubation for 24 h. Each value represents the mean ± SD ($n = 5$).

Acknowledgements

This work was supported by the National Natural Science Foundation of China (Grant no. 51173085 and 81000683) and PCSIRT (IRT 1257).

References

1 D. R. Owens, B. Zinman and G. B. Bolli, *Lancet*, 2001, **358**, 739–746.
2 K. M. Bratlie, R. L. York, M. A. Invernale, R. Langer and D. G. Anderson, *Adv. Healthcare Mater.*, 2012, **1**, 267–284.
3 V. Ravaine, C. Ancla and B. Catargi, *J. Controlled Release*, 2008, **132**, 2–11.
4 K. Kumareswaran, M. L. Evans and R. Hovorka, *Expert Rev. Med. Devices*, 2009, **6**, 401–410.
5 Z. Gu, A. A. Aimetti, Q. Wang, T. T. Dang, Y. L. Zhang, O. Veiseh, H. Cheng, R. S. Langer and D. G. Anderson, *ACS Nano*, 2013, **7**, 4194–4201.
6 Z. Gu, T. T. Dang, M. L. Ma, B. C. Tang, H. Cheng, S. Jiang, Y. Z. Dong, Y. L. Zhang and D. G. Anderson, *ACS Nano*, 2013, **7**, 6758–6766.
7 T. Miyata, T. Uragami and K. Nakamae, *Adv. Drug Delivery Rev.*, 2002, **54**, 79–98.

8 W. Qi, X. H. Yan, J. B. Fei, A. H. Wang, Y. Cui and J. B. Li, *Biomaterials*, 2009, **30**, 2799–2806.
9 K. Makino, E. J. Mack, T. Okano and W. K. Sung, *J. Controlled Release*, 1990, **12**, 235–239.
10 V. Lapeyre, I. Gosse, S. Chevreux and V. Ravaine, *Biomacromolecules*, 2006, **7**, 3356–3363.
11 K. Kataoka, H. Miyazaki, T. Okano and Y. Sakurai, *Macromolecules*, 1994, **27**, 1061–1062.
12 A. M. Horgan, A. J. Marshall, S. J. Kew, K. E. Dean, C. D. Creasey and S. Kabilan, *Biosens. Bioelectron.*, 2006, **21**, 1838–1845.
13 V. Lapeyre, C. Ancla, B. Catargi and V. Ravaine, *J. Colloid Interface Sci.*, 2008, **327**, 316–323.
14 D. Shiino, Y. Murata, A. Kubo, Y. J. Kim, K. Kataoka, Y. Koyama, A. Kikuchi, M. Yokoyama, Y. Sakurai and T. Okano, *J. Controlled Release*, 1995, **37**, 269–276.
15 A. Matsumoto, S. Ikeda, A. Harada and K. Kataoka, *Biomacromolecules*, 2003, **4**, 1410–1416.
16 B. L. Wang, R. J. Ma, G. Liu, Y. Li, X. J. Liu, Y. L. An and L. Q. Shi, *Langmuir*, 2009, **25**, 12522–12528.
17 T. Hoare and R. Pelton, *Macromolecules*, 2007, **40**, 670–678.
18 T. Hoare and R. Pelton, *Biomacromolecules*, 2008, **9**, 733–740.
19 V. Lapeyre, C. Ancla, B. Catargi and V. Ravaine, *J. Colloid Interface Sci.*, 2008, **327**, 316–323.
20 Y. J. Zhang, Y. Guan and S. Q. Zhou, *Biomacromolecules*, 2006, **7**, 3196–3201.
21 Y. J. Zhang, Y. Guan and S. Q. Zhou, *Biomacromolecules*, 2007, **8**, 3842–3847.
22 V. Lapeyre, I. Gosse, S. Chevreux and V. Ravaine, *Biomacromolecules*, 2006, **7**, 3356–3363.
23 A. Matsumoto, S. Ikeda, A. Harada and K. Kataoka, *Biomacromolecules*, 2003, **4**, 1410–1416.
24 A. Matsumoto, R. Yoshida and K. Kataoka, *Biomacromolecules*, 2004, **5**, 1038–1045.
25 Y. J. Lee, S. A. Pruzinsky and P. V. Braun, *Langmuir*, 2004, **20**, 3096–3106.
26 W. T. Wu, N. Mitra, E. C. Y. Yan and S. Q. Zhou, *ACS Nano*, 2010, **4**, 4831–4839.
27 A. Matsumoto, T. Ishii, J. Nishida, H. Matsumoto, K. Kataoka and Y. Miyahara, *Angew. Chem., Int. Ed.*, 2012, **51**, 2124–2128.
28 H. Kim, Y. J. Kang, S. Kang and K. T. Kim, *J. Am. Chem. Soc.*, 2012, **134**, 4030–4033.
29 C. Cheng, X. G. Zhang, Y. X. Wang, L. Sun and C. X. Li, *J. Mol. Catal. A: Chem.*, 2012, **36**, 1413–1421.
30 C. Zheng, Q. Q. Guo, Z. M. Wu, L. Sun, Z. P. Zhang, C. X. Li and X. G. Zhang, *Eur. J. Pharm. Sci.*, 2013, **49**, 474–482.
31 X. J. Jin, X. G. Zhang, Z. M. Wu, D. Y. Teng, X. J. Zhang, Y. X. Wang, Z. Wang and C. X. Li, *Biomacromolecules*, 2009, **10**, 1337–1345.
32 C. Cheng, X. G. Zhang, J. X. Xiang, Y. X. Wang, C. Zheng, Z. T. Lu and C. X. Li, *Soft Matter*, 2012, **8**, 765–773.
33 C. Cheng, X. G. Zhang, Y. X. Wang and C. X. Li, *J. Controlled Release*, 2011, **152**(suppl. 1), 267–269.
34 Y. X. Wang, X. G. Zhang, Y. C. Han, C. Cheng and C. X. Li, *Carbohydr. Polym.*, 2012, **89**, 124–131.
35 L. Sun, X. G. Zhang, C. Zheng, Z. M. Wu and C. X. Li, *J. Phys. Chem. B*, 2013, **117**, 3852–3860.
36 Z. M. Wu, X. G. Zhang, H. L. Guo, C. X. Li and D. M. Yu, *J. Mater. Chem.*, 2012, **22**, 22788–22796.
37 L. Sun, X. G. Zhang, C. Zheng, Z. M. Wu, X. T. Xia and C. X. Li, *RSC Adv.*, 2012, **2**, 9904–9913.
38 C. J. Ferguson, R. J. Hughes and D. Nguyen, *Macromolecules*, 2005, **38**, 2191–2204.
39 A. Aqil, H. Qiu and J. F. Greisch, *Polymer*, 2008, **49**, 1145–1153.
40 M. C. Lee, S. Kabilan, A. Hussain, X. P. Yang, J. Blyth and C. R. Lowe, *Anal. Chem.*, 2004, **76**, 5748–5755.
41 D. Roy, J. N. Cambre and B. S. Sumerlin, *Chem. Commun.*, 2008, **21**, 2477–2479.
42 Q. Yang, Z. K. Xu, Z. W. Dai, J. L. Wang and M. Ulbricht, *Chem. Mater.*, 2005, **17**, 3050–3058.
43 R. Narain and S. P. Armes, *Biomacromolecules*, 2003, **4**, 1746–1758.
44 M. M. Bradford, *Anal. Biochem.*, 1976, **72**, 248–254.
45 M. Sato, T. Furuike, R. Sadamoto, N. Fujitani, T. Nakahara, K. Niikura, K. Monde, H. Kondo and S. I. Nishimura, *J. Am. Chem. Soc.*, 2004, **126**, 14013–14022.
46 A. P. Bapat, D. Roy, J. G. Ray, D. A. Savin and B. S. Sumerlin, *J. Am. Chem. Soc.*, 2011, **133**, 19832–19838.
47 J. N. Cambre, D. Roy and B. S. Sumerlin, *J. Polym. Sci., Part A: Polym. Chem.*, 2012, **50**, 3373–3382.
48 S. Boduroglu, J. M. E. Khoury, D. V. Reddy, P. L. Rinaldi and J. Hu, *Bioorg. Med. Chem. Lett.*, 2005, **15**, 3974–3977.
49 S. Q. Li, E. N. Davis, J. Anderson, Q. Lin and Q. Wang, *Biomacromolecules*, 2009, **10**, 113–118.
50 R. J. Ma, H. Yang, Z. Li, G. Liu, X. C. Sun, X. J. Liu, Y. L. An and L. Q. Shi, *Biomacromolecules*, 2012, **13**, 3409–3417.
51 E. R. Ballister, A. H. Lai, R. N. Zuckermann, Y. Chenq and J. D. Mouqous, *Proc. Natl. Acad. Sci. U. S. A.*, 2008, **105**, 3733–3738.
52 R. A. Miller, A. D. Presley and M. B. Francis, *J. Am. Chem. Soc.*, 2007, **129**, 3104–3109.
53 T. Scheibel, R. Parthasarathy, G. Sawicki, X. M. Lin, H. Jaeqer and S. L. Lindquist, *Proc. Natl. Acad. Sci. U. S. A.*, 2003, **100**, 4527–4532.
54 W. T. Wu, N. Mitra, E. C. Y. Yan and S. Q. Zhou, *ACS Nano*, 2010, **4**, 4831–4839.
55 K. Hinds, J. J. Koh, L. Joss, F. Liu, M. Baudys and S. W. Kim, *Bioconjugate Chem.*, 2000, **11**, 195–201.
56 S. Lee, K. Kim, T. S. Kumar, J. Lee, S. K. Kim, D. Y. Lee, Y. K. Lee and Y. Byun, *Bioconjugate Chem.*, 2005, **16**, 615–620.

